The Journal of Neuroscience, August 1993, 13(8): 3252–3265

A Novel Slow (<1 Hz) Oscillation of Neocortical Neurons *in vivo*: Depolarizing and Hyperpolarizing Components

M. Steriade, A. Nuñez, and F. Amzica

Laboratoire de Neurophysiologie, Faculté de Médecine, Université Laval, Quebec, Canada G1K 7P4

We describe a novel slow oscillation in intracellular recordings from cortical association areas 5 and 7, motor areas 4 and 6, and visual areas 17 and 18 of cats under various anesthetics. The recorded neurons ($n = 254$) were antidromically and orthodromically identified as corticothalamic or callosal elements receiving projections from appropriate thalamic nuclei as well as from homotopic foci in the contralateral cortex. Two major types of cells were recorded: regular-spiking (mainly slow-adapting, but also fast-adapting) neurons and intrinsically bursting cells. A group of slowly oscillating neurons ($n = 21$) were intracellularly stained and found to be pyramidal-shaped cells in layers III–VI, with luxuriant basal dendritic arbors.

The slow rhythm appeared in 88% of recorded neurons. It consisted of slow depolarizing envelopes (lasting for 0.8–1.5 sec) with superimposed full action potentials or presumed dendritic spikes, followed by long-lasting hyperpolarizations. Such sequences recurred rhythmically at less than 1 Hz, with a prevailing oscillation between 0.3 and 0.4 Hz in 67% of urethane-anesthetized animals.

While in most neurons (≈70%) the repetitive spikes superimposed on the slow depolarization were completely blocked by slight DC hyperpolarization, 30% of cells were found to display relatively small (3–12 mV), rapid, all-or-none potentials after obliteration of full action potentials. These fast spikes were suppressed in an all-or-none fashion at V_m more negative than −90 mV. The depolarizing envelope of the slow rhythm was reduced or suppressed at a V_m of −90 to −100 mV and its duration was greatly reduced by administration of the NMDA blocker ketamine. In keeping with this action, most (56%) neurons recorded in animals under ketamine and nitrous oxide or ketamine and xylazine anesthesia displayed the slow oscillation at higher frequencies (0.6–1 Hz) than under urethane anesthesia (0.3–0.4 Hz).

In 18% of the oscillating cells, the slow rhythm mainly consisted of repetitive (15–30 Hz), relatively short-lasting (15–25 msec) IPSPs that could be revealed by bringing the V_m at more positive values than −70 mV. The long-lasting (≈1 sec) hyperpolarizing phase of the slow oscillation was best observed at the resting V_m and was reduced at about −100 mV. Simultaneous recording of another cell across the membrane demonstrated synchronous inhibitory periods in both neurons. Intracellular diffusion of Cl^- or Cs^+ reduced the amplitude and/or duration of cyclic long-lasting hyperpolarizations.

Thus, the newly described oscillation is present in all investigated (sensory, motor, and associational) cortical areas, is displayed by morphologically and physiologically identified pyramidal cells, but does also seemingly involve local-circuit inhibitory cells as inferred from the rhythmic (0.3 Hz) sequences of repetitive IPSPs in pyramidal-type neurons. We then deal with a massive population event, as also indicated by the close correlation between the slow cellular and EEG oscillation. As shown in the following two companion articles (Steriade et al., 1993a,b), the slow cortical oscillation survives total lesions of thalamic perikarya projecting to the recorded cortical neurons and plays a pivotal role in grouping within the 0.3 Hz rhythm other sleep oscillations, such as spindle (7–14 Hz) and delta (1–4 Hz) waves. A new view of sleep oscillations emerges, with various cerebral rhythms generated by intrinsic electrophysiological properties of thalamic and cortical neurons and by synaptic interactions in complex corticothalamocortical networks.

[Key words: neocortex, thalamus, sleep, anesthesia, slow rhythm, intracellular recordings, dendritic spikes, depolarizations, hyperpolarizations]

The oscillations occurring during the state of quiescent sleep have been intensively studied since the 1930s at the gross level of the EEG. Two major EEG rhythms are usually described in animals and humans during this behavioral state associated with loss of perceptual awareness: spindles during the early stages, and delta waves during later stages of sleep (Steriade et al., 1990a). While performing studies of thalamic and cortical neurons aimed at revealing the cellular bases of oscillations within the frequency band of 0.1–4 Hz, we recently realized that these rhythms do not constitute a homogeneous entity. Instead, they belong to at least two different types of oscillatory activities (1–4 Hz, hereafter termed delta rhythm, and <1 Hz, hereafter termed slow rhythm), with distinct sites of genesis and dissimilar mechanisms. The first aim of this series of articles is to describe a newly discovered slow oscillation (usually between 0.2 and 0.5 Hz) of intracellularly recorded neocortical neurons under different anesthetics. As shown in Figure 1, this slow oscillation is also present in the EEG of naturally sleeping cats and humans and it consists of periodically recurring sequences of EEG delta

Received Oct. 1, 1992; revised Jan. 15, 1993; accepted Feb. 18, 1993.

This work was supported by Medical Research Council of Canada Grant MT-3689. A.N. was a postdoctoral fellow supported by the Spanish Department of Education and Science. F.A. is a doctoral student. We thank our colleagues D. Paré and D. Contreras for helpful discussions and remarks on an earlier version of the manuscript, G. Oakson for providing the analysis software, and P. Giguère and D. Drolet for technical assistance.

Correspondence should be addressed to Prof. Dr. M. Steriade, Laboratoire de Neurophysiologie, Département de Physiologie, Faculté de Médecine, Université Laval, Quebec, Canada G1K 7P4.

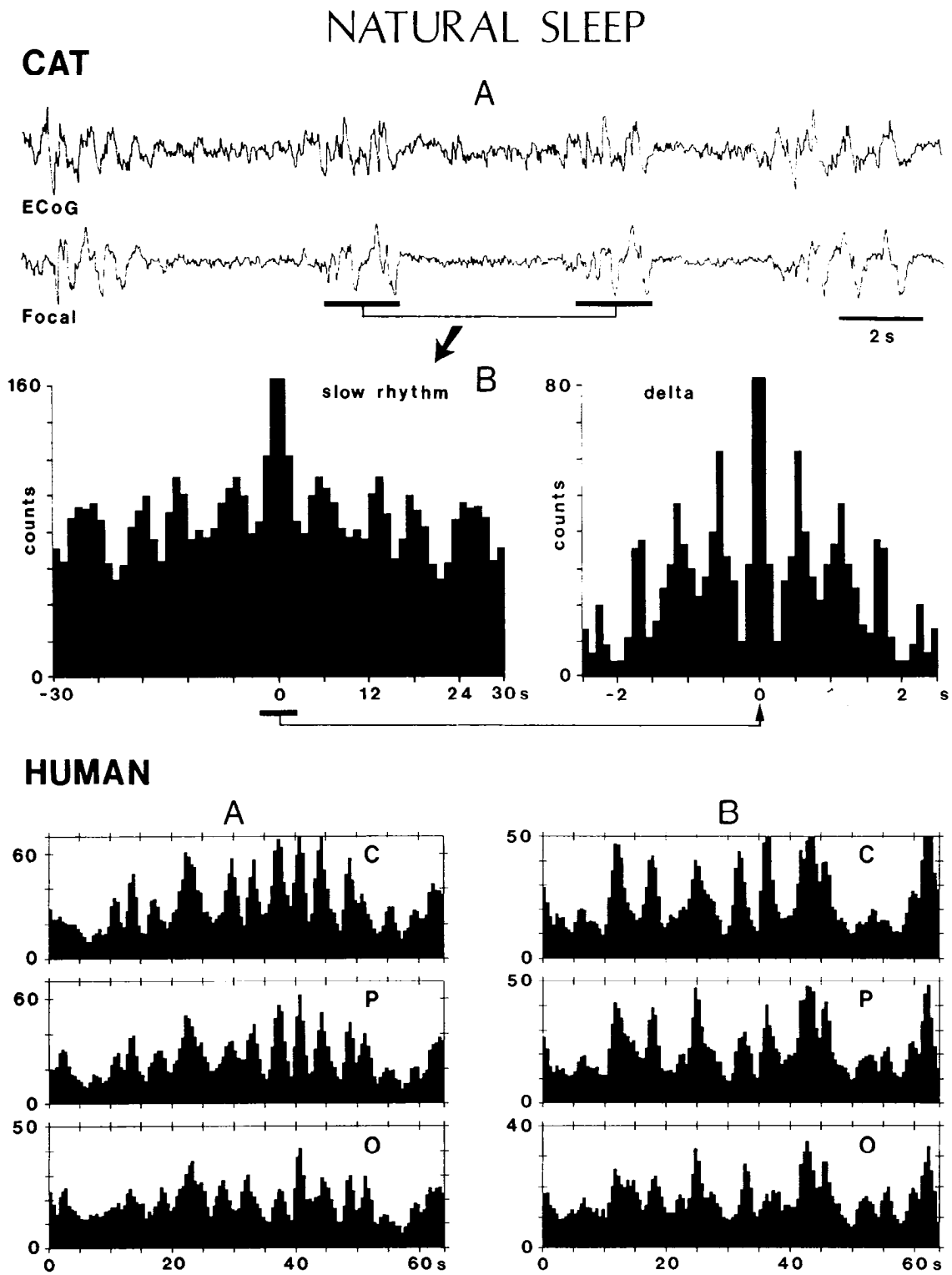

Figure 1. The slow (0.15–0.25 Hz) rhythm of cortical EEG waves during natural sleep in cat and human. At the *top*, *A* shows ECoG waves recorded from a chronically implanted behaving cat, through a silver ring placed on the surface of suprasylvian area 5 (*upper trace*), and focal waves simultaneously recorded by a tungsten microelectrode inserted through the ring to a depth of 1.2 mm (*bottom trace*). *B* depicts autocorrelograms computed with bins of 1 sec (*left*) and 0.1 sec (*right*) from a period of 2 min, of which the shorter period in *A* is illustrated. The slow rhythm of delta wave sequences is marked by two *horizontal bars*. Detected events were high-amplitude waves (central peaks in both histograms are cut). Note the slow rhythm (0.15–0.2 Hz) in *left histogram*, and delta waves (1–1.5 Hz) in *right histogram* representing an expanded part of the portion marked by a *bar* in the *left histogram*. At the *bottom*, in the human scalp recordings (*A* and *B* are from two adult normal subjects), EEG epochs from sleep stages 3–4 were filtered to 0.5–4 Hz and the sequential mean amplitude was computed by calculating the root mean square voltage in μV (*ordinate*) for sequential periods of 0.5 sec. The result was then smoothed with a three-bin unweighted moving average. *C*, *P*, and *O*, central, parietal, and occipital leads of the same hemisphere. Note in both cases sequences of delta waves recurring periodically with a slow rhythm of 0.15–0.2 Hz, quite similar to the above data from cat. Unpublished data by F. Amzica and M. Steriade (*Cat*) and by G. Oakson and M. Steriade (*Human*).

waves. With the benefit of hindsight, these aspects may also be seen in previous EEG recordings of humans and experimental animals (see Discussion).

During the past decade, progress has been made to understand the neuronal substrates of spindles (7–14 Hz). It was shown that these oscillations are generated by intrinsic and synaptic properties of thalamic neurons and that the reticular (RE) thalamic neurons have a key role in their synchronization (see Steriade et al., 1990b). More recently, an oscillation within the frequency range of EEG delta waves (1–4 Hz), due to the interplay between two intrinsic currents of thalamocortical neurons, was described both *in vitro* (McCormick and Pape, 1990; Leresche et al., 1991) and *in vivo* (Steriade et al., 1991; Curró Dossi et al., 1992). However, the clocklike, stereotyped delta oscillation of single thalamic cells is dissimilar from the irregular, polymorphous EEG delta waves during natural sleep or anesthesia. Besides, while rhythmic events within the delta frequency range are intrinsically generated in thalamic neurons, this activity cannot reach the cortex to be reflected at the macroscopic EEG level unless thalamic neurons are synchronized (Steriade et al., 1991).

In this article, we describe the novel, depolarizing–hyperpolarizing oscillation (≈0.3 Hz) of morphologically and physiologically identified, pyramidal-shaped neocortical neurons projecting to the thalamus and/or the contralateral cortex. We began the experiments by recording the activity of neurons in association areas 5 and 7, because our previous studies on delta rhythmicity (Steriade et al., 1991; Curró Dossi et al., 1992) were mainly conducted in thalamic nuclei projecting to those cortical areas, that is, lateroposterior (LP) and rostral intralaminar centrolateral (CL) nuclei. Subsequent recordings in other cortices, such as the visual and motor areas, provided evidence that the slow oscillation is generalized at the level of the neocortex. In the following companion articles (Steriade et al., 1993a,b), we analyze the relations between the slow cortical oscillation and other sleep rhythms (spindles and delta) as well as the close time relation between the slow cortical oscillation and the gross EEG activity recorded from the cortex and the thalamus; we report the presence of a similar slow rhythm in RE thalamic and thalamocortical cells; and we propose a scenario for the genesis of major sleep rhythms in interacting corticothalamocortical networks.

Materials and Methods

Experiments were conducted on 57 adult cats. (1) Of those, 30 were anesthetized with urethane (1.8 gm/kg, i.p.). Additional doses of the same anesthetic (0.2–0.5 gm/kg) were administered at the slightest sign of diminished amplitude and increased frequency of EEG waves. Thus, a constant pattern of EEG synchronization was maintained throughout the experiments. Twenty other animals were investigated by using ketamine (40 mg/kg, i.m.) supplemented with nitrous oxide ($n = 12$), or ketamine (10–15 mg/kg, i.m.) and xylazine (2–2.5 mg/kg) ($n = 8$); these anesthetics were repeated to maintain a permanent picture of EEG synchronization. Deep anesthesia with sodium pentobarbital (35 mg/kg, i.p.) was used in three animals. The remaining four animals were investigated to obtain recordings in the *cerveau isolé* (isolated forebrain) preparation, without large doses of anesthetics (see Steriade et al., 1993a). (2) Occasionally, the short-acting barbiturate sodium thiamylal (2–4 mg/kg, i.v.) or small doses of ketamine were injected in urethane-anesthetized animals to study the changes in cellular and EEG aspects of the slow oscillation. In addition to general anesthetics or to brainstem transection, the tissues to be incised and pressure points were infiltrated before surgery with lidocaine.

All animals were paralyzed with gallamine triethiodide and artificially ventilated with control of the end-tidal CO_2 concentration at 3.7 ± 0.2%. Internal temperature (37–38°C) and heartbeat were continuously monitored. The stability of recordings was ensured by bilateral pneumothorax, cisternal drainage, hip suspension, and by filling the hole made in the calvarium with 4% agar dissolved in saline.

Intracellular recordings were performed with micropipettes (tip diameter, 0.5 μm) filled with 3 M solution of K-acetate or 1–3 M KCl (DC resistance 25–40 MΩ), with 0.5–1 M Cs-acetate (35–50 MΩ), or with 0.03–0.1 M QX-314 (40–60 MΩ). Unless otherwise specified, the depicted cells were recorded with micropipettes filled with K-acetate. Also, micropipettes filled with 3% Lucifer yellow (LY) in 1 M LiCl (DC resistance, 30–60 MΩ) were used for the morphological identification of the oscillating neurons. LY was injected by passing hyperpolarizing current pulses (0.5 sec, 1–2 nA) at 1 Hz, for ≈10–20 min. A high-impedance amplifier with active bridge circuitry was used to record and inject current inside the cells. The signals were digitally recorded on tape (bandpass, DC to 9 kHz) and data were fed in a computer with sample rate of 20 kHz for off-line analysis. The laminar location of neurons was estimated from micromanipulator readings along tracks perpendicular to the cortical surface. These measurements were compared with the position of LY-stained neurons; differences were less than 15%.

The gross electrical activity was routinely recorded throughout the experiments, either as electrocorticogram (ECoG) from stainless steel screws into the ipsilateral calvarium at ≈3 mm apart from the site of intracellular recordings, or as ECoG from the homotopic contralateral cortical area, or as electrothalamogram (EThG) by using the electrodes inserted in appropriate thalamic nuclei for stimulation purposes.

Stimulating electrodes (either bipolar, made of used tungsten microelectrodes, or coaxial) were inserted in thalamic nuclei having reciprocal connections with the investigated cortical area: LP and CL in the case of recordings from suprasylvian areas 5 and 7, ventroanterior–ventrolateral complex when recordings were made in pericruciate motor areas 4 and 6, and dorsal lateral geniculate nucleus (dLGN) when recordings were made from visual areas 17 and 18 in the marginal gyrus. In addition, coaxial electrodes were inserted in the depth of the homotopic cortical areas of the contralateral hemisphere. Stimulation consisted of current pulses (duration of 0.05–0.3 msec) of various intensities, usually ranging from 0.05 to 0.4 mA.

At the end of experiments, the animals were deeply anesthetized with a lethal dose of sodium pentobarbital (50 mg/kg). After experiments with LY injections and/or thalamic lesions, the animals were perfused transcardially with saline followed by 10% paraformaldehyde. The location of stimulating thalamic electrodes and the size of brainstem and thalamic lesions were verified on 40–75 μm frontal or sagittal sections stained with thionine. Sections with LY-stained cells (75 μm) were observed and photographed with a camera fixed to a fluorescence microscope.

Results

Data base, general properties, and physiological identification

We have recorded 254 neurons intracellularly and 23 neurons extracellularly. Of those, 233 cells were recorded in suprasylvian areas 5 and 7, 25 cells in pericruciate areas 4 and 6, and 19 cells in areas 17 and 18 of the marginal gyrus, as defined in cytoarchitecture studies of cat neocortex (Gurewitsch and Chatschaturian, 1928; Hassler and Muhs-Clement, 1964).

The neurons recorded intracellularly had membrane potential (V_m) more negative than −60 mV and overshooting action potentials. In a representative sample of 82 cells, the V_m (without current) was −70.7 ± 0.6 mV (mean ± SE; range, −60 to −83 mV), the amplitude of action potentials was 82.1 ± 0.9 mV (range, 65–100 mV), and the input resistance (measured through hyperpolarizing current pulses, 40–50 msec, <1 nA) was 20.6 ± 0.7 MΩ (range, 10–40 MΩ). In all figures depicting oscillating neurons with pronounced hyperpolarizations, the indicated V_m represents the trough between the depolarizing episodes.

Two major types of cells were recorded: regular-spiking and intrinsically bursting neurons. The features of these neuronal classes, described in cortical slices from animals and humans (Connors et al., 1982; McCormick et al., 1985; Stafstrom et al., 1985; Avoli and Olivier, 1989; Foehring et al., 1991), are reported in a parallel *in vivo* study on cat association neurons

recorded from areas 5 and 7 (Nuñez et al., 1993). The neurons displaying the slow oscillation described in this and companion articles belonged to both regular-spiking (mainly slowly, but also fast-adapting) and intrinsically bursting cell classes, as indicated in the captions of different figures. We did not record fast-spiking, probably inhibitory cells (McCormick et al., 1985).

Physiological identification of input–output organization of recorded cells was achieved by means of thalamic and cortical stimulation. The same neuron could be synaptically driven from both LP and CL thalamic nuclei as well as from the contralateral cortex. Thalamic and cortical converging inputs were seen in 35% of tested neurons. At the resting V_m, the cell depicted in Figure 2*A* displayed a stereotyped spike-doublet in response to either LP or cortical stimulus, with an inflection on the rising phase of the full action potential. DC hyperpolarization revealed partial spikes with the same latencies. At a V_m more negative than −90 to −105 mV, these all-or-none events were blocked and replaced by a smooth depolarization. They were clearly distinct from the EPSPs on the basis of their shorter duration (1.5–3 msec) and much faster rising slopes as well as their blockage by hyperpolarization. While the origin of such cortical fast prepotentials (FPPs) cannot be resolved in our *in vivo* preparation, these FPPs might represent dendritic spikes. As shown below, neurons with presumed dendritic spikes displayed the slow oscillation (see Fig. 4).

The antidromic responses had a fixed latency, took off from the baseline, and could follow stimuli at fast frequencies (Fig. 2*B,C*). Latencies of thalamically evoked antidromic responses (in layers VI and V) ranged from 1 to 6 msec (mean, 2.9 ± 0.3 msec and 2.8 ± 0.5 msec for LP and CL stimulation, respectively). Latencies of cortically elicited antidromic spikes (in layers II–IV) ranged between 1 and 4 msec (mean, 1.4 ± 0.3 msec). DC hyperpolarization blocked antidromic responses and revealed EPSPs (Fig. 2*B,C*). Similar antidromic spikes and EPSPs were observed in motor and visual cortices (see Fig. 9), although the numbers of recorded cells in those areas were smaller.

Thus, ortho- and antidromic identification of neurons revealed their involvement in reciprocal corticothalamic and corticocortical (callosally mediated) pathways.

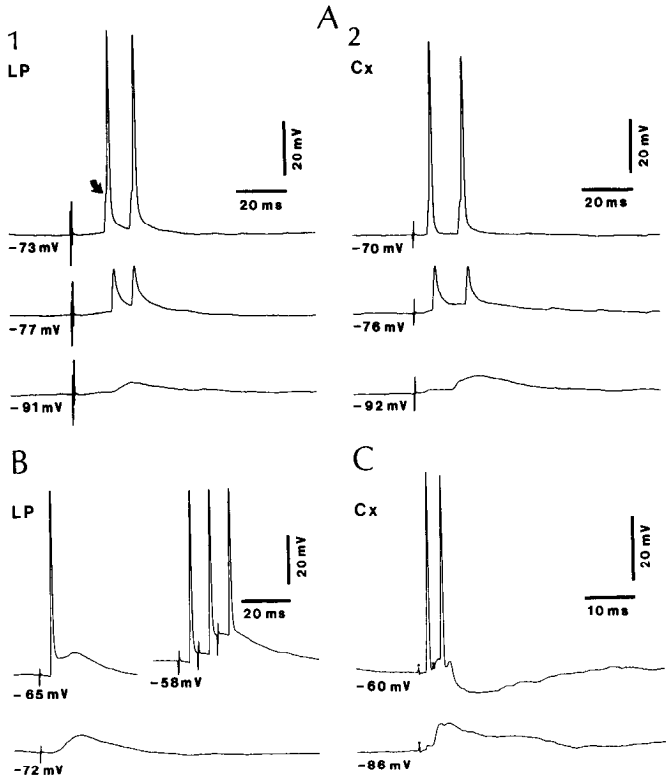

Figure 2. Physiological identification of neurons in cortical association areas 5 and 7. *A–C* are from three regular-spiking, slowly adapting cells. *A*, Neuron recorded at a depth of 1.1 mm in area 5, synaptically driven from both LP thalamic nucleus (*1*; latency, 14 msec) and homotopic area in the contralateral suprasylvian cortex (*2*; latency, 5 msec). *B*, Cell recorded at 1.3 mm in area 7, antidromically activated from LP nucleus (latency, 4.3 msec). *C*, Neuron recorded at 0.5 mm in area 7, backfired from the contralateral cortex (latency 1.5 msec). In this and following figures, V_m is indicated.

General description of slow oscillation

In most neurons, the slow oscillation consisted of long-lasting depolarizations, with superimposed full somatic action potentials or presumed dendritic spikes, separated by long periods of neuronal silence (Figs. 3, 4). Less often, the phasic depolarizing events were reversed IPSPs (see Fig. 6). Finally, in other slowly oscillating cells, the major events were pronounced hyperpolarizations that periodically sculptured the neuronal firing (see Fig. 7). In fact, the slow oscillation probably included EPSPs and IPSPs as well as intrinsic currents, the predominance of one or another aspect varying from cell to cell according to their place in the circuitry and to our ability in revealing these components (see Discussion). For the sake of clarity, experimental data will be presented by taking into consideration different neuronal classes.

As shown in Figure 6*B* and as fully described in the next article, the slow cellular oscillation was closely related with a similar rhythm of EEG waves.

The slow oscillation, with some or all the above features, was observed in 88% of recorded neurons, under all (but deep barbiturate) anesthetic conditions, as well as in high brainstem-transected (*cerveau isolé*) undrugged preparations. The basic difference between neuronal oscillations recorded under urethane and those under ketamine (the latter supplemented with nitrous oxide or xylazine) was the frequency of the rhythm. In a sample of 133 neurons recorded intracellularly under urethane anesthesia, the frequency mode (in 67% of cells) was between 0.3 and 0.4 Hz. The remaining oscillatory neurons displayed frequencies at <0.1 Hz (15.8%) or 0.1–0.2 Hz (10.5%), with only 6.5% of cells oscillating at frequencies between 0.4 and 1 Hz. Distinctly, in a sample of 14 neurons recorded under ketamine anesthesia, 21.5% oscillated at <0.1 Hz, 22.5% oscillated between 0.2 and 0.5 Hz, and 56% had oscillation frequencies ranging between 0.6 and 1 Hz, that is, a pronounced shift toward higher frequencies. As shown in Figure 5, this was due to the ketamine-induced diminution in the duration of depolarizing envelopes and interdepolarization lulls. Deep barbiturate anesthesia produced an overwhelming pattern of spindling activity (see next article).

The depolarizing component, somatic action potentials, and dendritic spikes

In regular-spiking cells recorded under urethane anesthesia, which generally oscillated at 0.3–0.4 Hz, the depolarizing phase lasted for 0.8–1.5 sec and gave rise to repetitive single spikes at frequencies varying from 5 to 30 Hz, depending on the V_m (Fig. 3*A,B*). The participation of intrinsically bursting cortical cells in the 0.3 Hz rhythm is reported in the following article (see

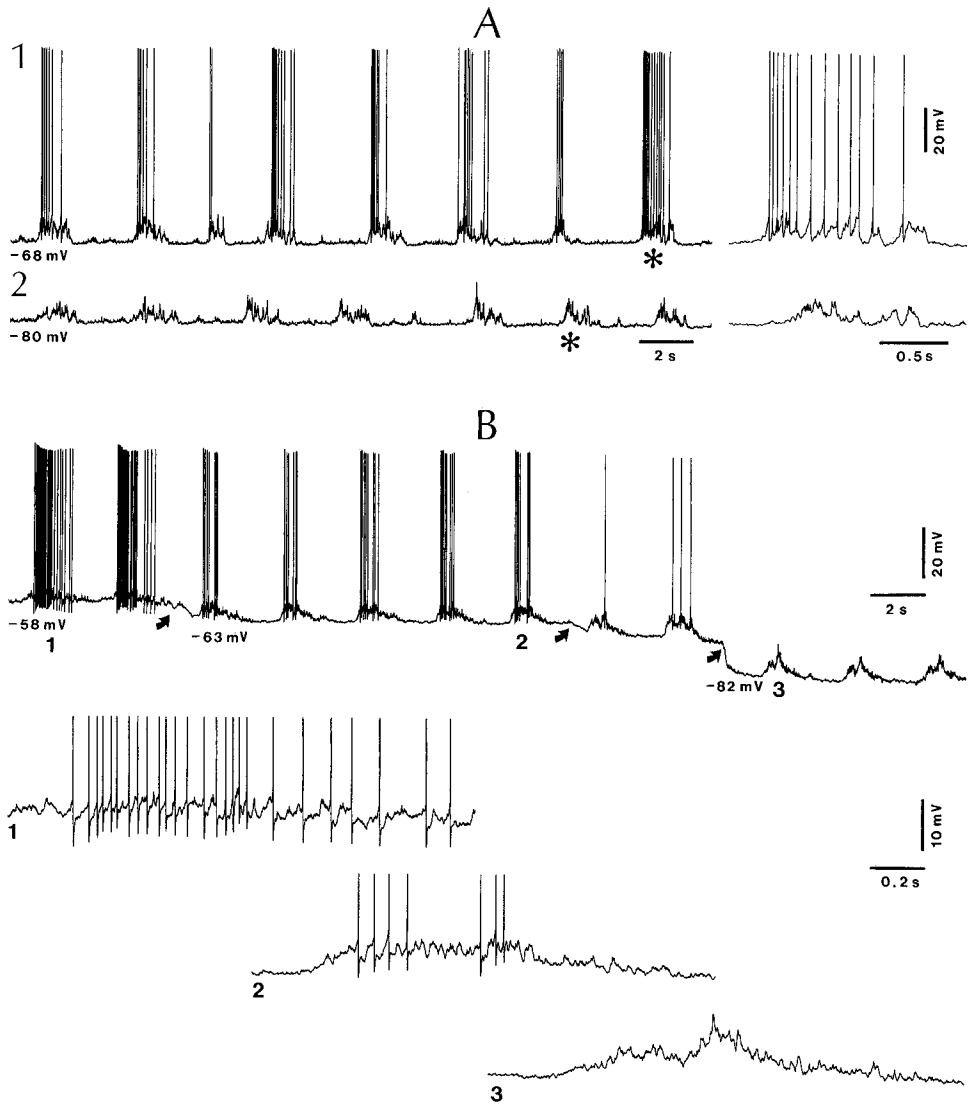

Figure 3. The slow (≈0.3–0.4 Hz) depolarizing oscillation: two regular-spiking, slowly adapting neurons. *A*, Cell recorded at 0.8 mm in area 5, synaptically driven at 1.5 msec from the LP nucleus: *1*, activity at the resting V_m (−68 mV); *2*, under DC hyperpolarization (−1 nA). Depolarizing envelopes marked by *asterisks* are expanded at *right*. *B*, Cell recorded at 1.3 mm in area 7 (same neuron as depicted with antidromic identification in Fig. 2*B*). *From left to right*, Under DC depolarization (−58 mV, +0.4 nA); removal of current (*oblique arrow*, bringing the V_m at rest (−63 mV); and two steps of DC hyperpolarization (*two oblique arrows*). Depolarizing envelopes marked by *1–3* are expanded below (spikes truncated).

Figs. 6, 7, 11*A*, 14 in Steriade et al., 1993a), mainly in relation to the persistence of this slow oscillation in athalamic preparations.

Slight DC hyperpolarization blocked the action potentials, enhanced the amplitude of the depolarizing envelope, and produced an increase in synaptic noise (Fig. 3*B*, 1–3). Further hyperpolarization, however, eventually blocked the slow oscillation in a population of 22 neurons (see Fig. 4*B*).

Whereas in 70% of neurons DC hyperpolarization completely blocked the spikes superimposed on the slow depolarization, the remaining oscillating cells exhibited relatively small (3–12 mV), rapid, all-or-none events after obliteration of full action potentials by slight hyperpolarization. We hypothesize that these FPPs are dendritic spikes. Indeed, they had a time to peak and a rising slope much faster and more abrupt than the EPSPs, could be elicited by depolarizing pulses, and were blocked in an all-or-none fashion by DC hyperpolarization beyond −90 or −100 mV (Fig. 4*C*). Alternatively, the fast events may be initial segment spikes or may be ascribed to gap junctions. However, gap junctions are rare in adult animals (see Discussion). In the corticothalamic neuron depicted in Figure 4*A*, the repetitive all-or-none potentials were the most prominent events of the depolarizing envelope. Both fast and slow oscillatory events disappeared or were reduced at −100 mV, and they reappeared around the resting V_m (Fig. 4*B*). Similar fast events were elicited by synaptic stimulation (Fig. 4*C*).

Reduction of slow depolarization by QX-314 or ketamine

The prolonged duration of the depolarizing envelope and its almost suppression at hyperpolarized levels (Fig. 4), despite the persistence and even the increase of short-lasting excitatory potentials, suggested that at least two nonexclusive factors contribute to this slow event: (1) one could be a persistent Na^+ current ($g_{Na(p)}$), triggered by EPSPs from synaptic activities in cortical networks; and (2) the other possible factor involved in the long-lasting depolarization may be the voltage-dependent, prolonged, NMDA-mediated EPSP.

While we observed that the slow depolarizing envelope was drastically diminished after impalements with micropipettes filled with QX-314 (data not shown), this is a nonspecific antagonist of $g_{Na(p)}$ and we could not precisely determine the participation of this conductance in the slow depolarization.

As indicated above (see General description of slow oscillation), most neurons under urethane anesthesia oscillated at 0.3–

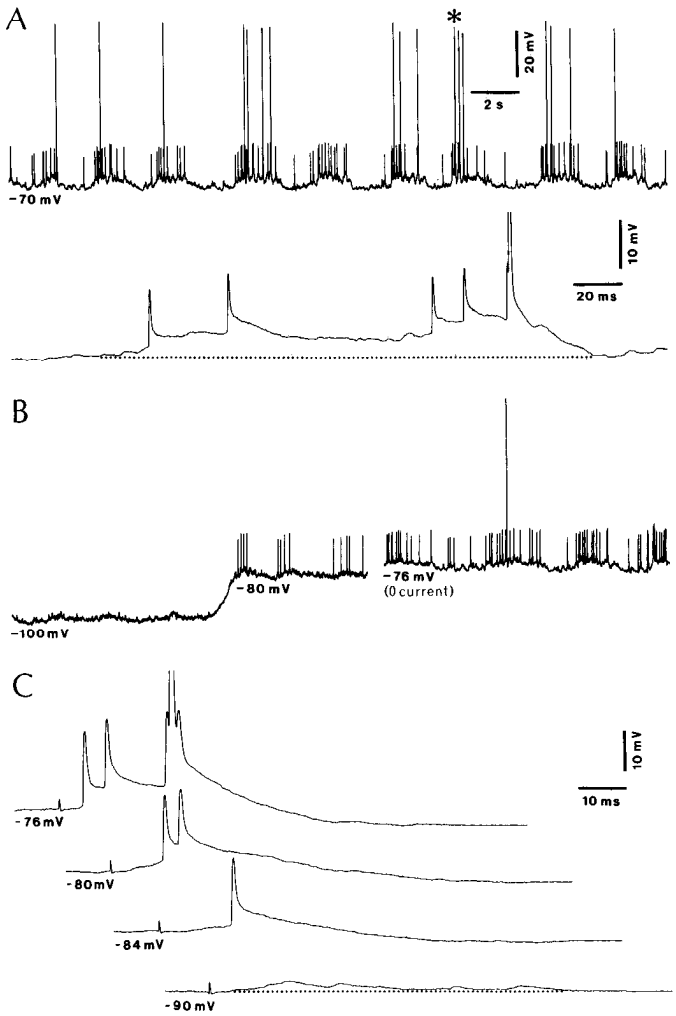

Figure 4. Blockage of presumed dendritic spikes and reduction of rhythmic (≈0.3 Hz) depolarizing envelopes under DC hyperpolarization: regular-spiking, slowly adapting cell recorded at 1.4 mm in area 5 (backfired from LP nucleus and orthodromically activated from CL nucleus). Resting V_m was −76 mV (see *right part* in *B*). *A*, Under DC depolarization (+0.3 nA). Episode marked by *asterisk* is expanded below to show the buildup of the depolarizing envelope (*dotted line* tentatively indicates the baseline). *B*, Unitary events and depolarizing envelopes were virtually blocked at −100 mV. At *right*, recovery of slow rhythm by removing the DC hyperpolarizing current. *C*, Presumed dendritic spikes evoked by CL stimulation at different V_m. Note underlying slow EPSP at −90 mV.

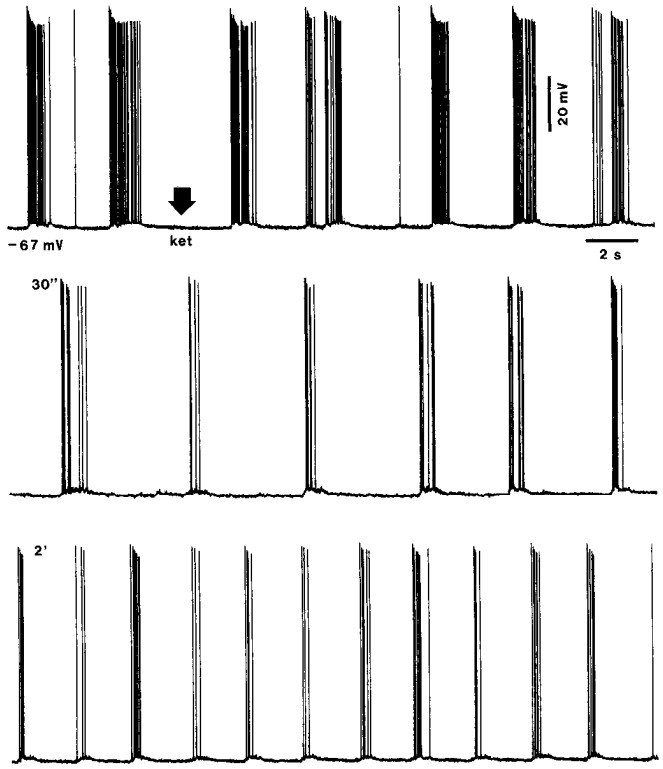

Figure 5. Effect of ketamine upon the slow (≈0.3 Hz) oscillation of regular-spiking, slow-adapting area 5 neuron under urethane anesthesia. Ketamine (2.5 mg/kg) was administered intravenously at *arrow*. No changes in V_m were observed at 30 sec and 2 min, depicted below. Note progressive reduction in duration of rhythmic depolarizing envelopes (*30"*) and, subsequently (*2'*), increased frequency of the slow rhythm.

0.4 Hz, whereas the majority of neurons recorded under ketamine anesthesia (supplemented with either nitrous oxide or xylazine) oscillated at higher frequencies, 0.6–1 Hz. The frequency transformation of the slow oscillation, from 0.3 to more than 0.5 Hz, was obtained in the same neuron by intravenous administration of very small (<3–4 mg/kg) doses of ketamine in already urethane-anesthetized animals ($n = 21$). Since the initial description of the NMDA-mediated EPSP (Thomson, 1986), it is known that ketamine and other dissociative anesthetics selectively block the NMDA subtype of excitatory amino acid receptor (MacDonald et al., 1991). Thirty seconds after injection of 2.5 mg/kg ketamine, the prolonged (>1 sec) depolarization of the neuron illustrated in Figure 5 was progressively reduced to 0.3–0.5 sec and, correlatively, the number of action potentials decreased by more than half. The duration of the interdepolarizing lulls also decreased and the frequency of the oscillation increased from 0.2–0.3 Hz to 0.5 Hz.

Slow oscillations made by repetitive IPSPs

In some of the neurons presented above, the slow depolarizing envelopes were not exclusively associated with EPSPs, but also with hyperpolarizing events having short duration and clearly visible at relatively depolarized levels. We then hypothesized that, in addition to the rhythmic excitatory impingement from ipsi- and contralateral cortical neurons, the recorded cells were also the target of local-circuit inhibitory cells oscillating at similar frequencies.

In 18% of oscillating neurons ($n = 44$), we succeeded in revealing that the slow rhythm consists of repetitive IPSPs grouped in periodic sequences. This disclosure was made possible by using steady depolarizing currents, bringing the V_m at more positive values than −70 mV. Two of these cells are depicted in Figure 6. At the resting V_m, the neuron in Figure 6*A* displayed rhythmic (≈0.25 Hz) depolarizing envelopes, with fast (≈30 Hz), short-duration (15–25 msec) depolarizing wavelets. These fast events became hyperpolarizing and preserved their frequencies under DC depolarization to −65 mV. The other cell (Fig. 6*B*) oscillated at 0.35 Hz. Similarly, sequences of brief (≈30 msec) IPSPs appeared when the V_m was changed from rest (−80 mV) to −66 mV. Because the latter neuron displayed repetitive IPSPs at around 15 Hz, we wondered whether or not these inhibitory events reflect the synaptic engagement of local-circuit inhibitory cortical cells driven by spindle oscillations arising in the afferent thalamocortical projection. The simul-

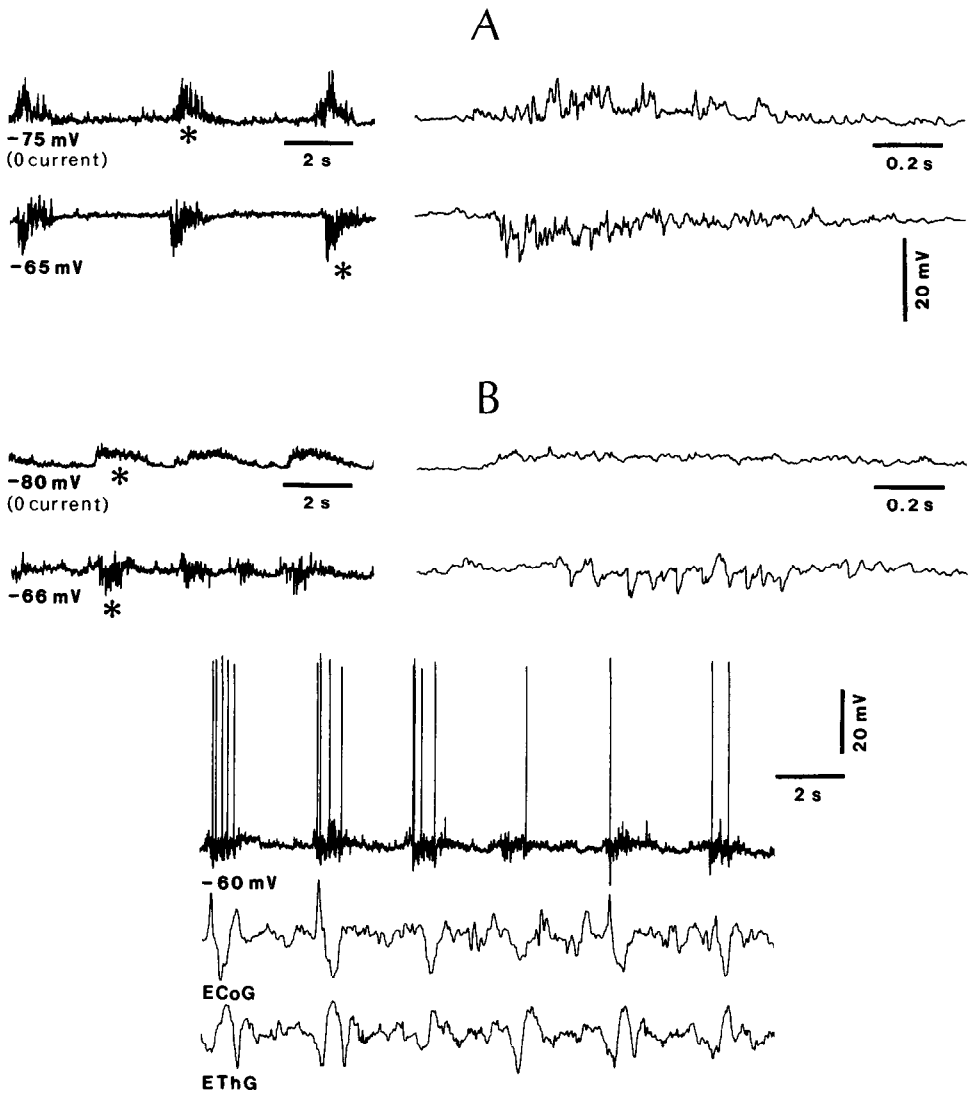

Figure 6. Slow (≈0.25–0.35 Hz) rhythms made up by sequences of repetitive IPSPs. *A*, Cell recorded at 0.6 mm in area 5, synaptically driven from the LP nucleus and contralateral area 7. At rest (−75 mV), the oscillation consisted of rhythmic (0.2–0.25 Hz) depolarizations. IPSPs were revealed by DC depolarization (+0.6 nA), bringing the V_m to −65 mV. Episodes marked by *asterisks* are expanded at *right*. *B*, Cell recorded at 0.9 mm in area 7, synaptically driven from LP nucleus. Rhythmic (0.3–0.4 Hz) depolarizations at rest (−80 mV) and sequences of IPSPs revealed by DC depolarization (+1.6 nA), bringing the V_m to −66 mV. Episodes marked by *asterisks* are expanded at *right*. *Bottom*, Under further DC depolarization (−60 mV), slow rhythm with occasional spike discharges; *below*, the simultaneous recording of the ipsilateral ECoG from area 5 and EThG in LP nucleus.

taneously recorded ECoG and EThG indicated that this was *not* the case. Indeed, the slow (0.35 Hz) oscillation occurred in close time relation with complexes of slow and large-amplitude EEG waves, but spindles were not apparent (see bottom part of Fig. 6*B*). The following article (Steriade et al., 1993a) provides additional evidence that the novel slow oscillation does appear in experimental conditions, such as deep urethane anesthesia, in which spindle sequences are scarce and are not grouped in clear-cut sequences at 0.1–0.2 Hz.

Long-lasting hyperpolarizations sculpturing the slow oscillation

In 22% of neurons (n = 53), the slow oscillation essentially consisted of long-lasting (up to 1 sec) hyperpolarizations, with amplitudes of 7–10 mV, which recurred periodically and sculptured the neuronal firing. This oscillatory type was best observed at the resting V_m (−70 mV) when action potentials did not occur. DC hyperpolarization to −100 mV reduced the amplitude and duration of hyperpolarization.

In a few instances (n = 3), we were able to record simultaneously across the membrane another cell of the same type. The inhibitory phases of the oscillation were clearly synchronized in both cells. In Figure 7, the intracellularly recorded neuron displayed prevailing hyperpolarizations (≈1 sec in duration), recurring periodically every 2–2.5 sec and associated with a decrease in synaptic noise. The episodes between hyperpolarizations began with a steep depolarizing event, occasionally leading to a single action potential. The extracellularly recorded cell discharged tonically (3–4 Hz) and its rhythmic periods of silenced firing coincided (in both onset and duration) with the hyperpolarizations of the impaled neuron. Cross-correlograms of activities in both cells confirmed the synchronizing inhibitory process (Fig. 7).

We recorded 17 neurons with KCl-filled pipettes to assess the contribution of $GABA_A$-mediated Cl^--dependent IPSPs to the slow oscillation. In 14 of those tested cells, the hyperpolarizations were decreased in their amplitudes and/or duration (Fig. 8). The effect of Cs^+ on K^+ currents, presumably involved in the genesis of long-lasting hyperpolarizations, was tested in seven neurons that all displayed a reduced amplitude of hyperpolarizations a few min after impalement (data not shown).

The slow oscillation in motor and visual cortices

A similar pattern of slowly recurring depolarizing envelopes interrupted by long-lasting hyperpolarizations, leading to a slow rhythm as described above in associational areas, was seen in

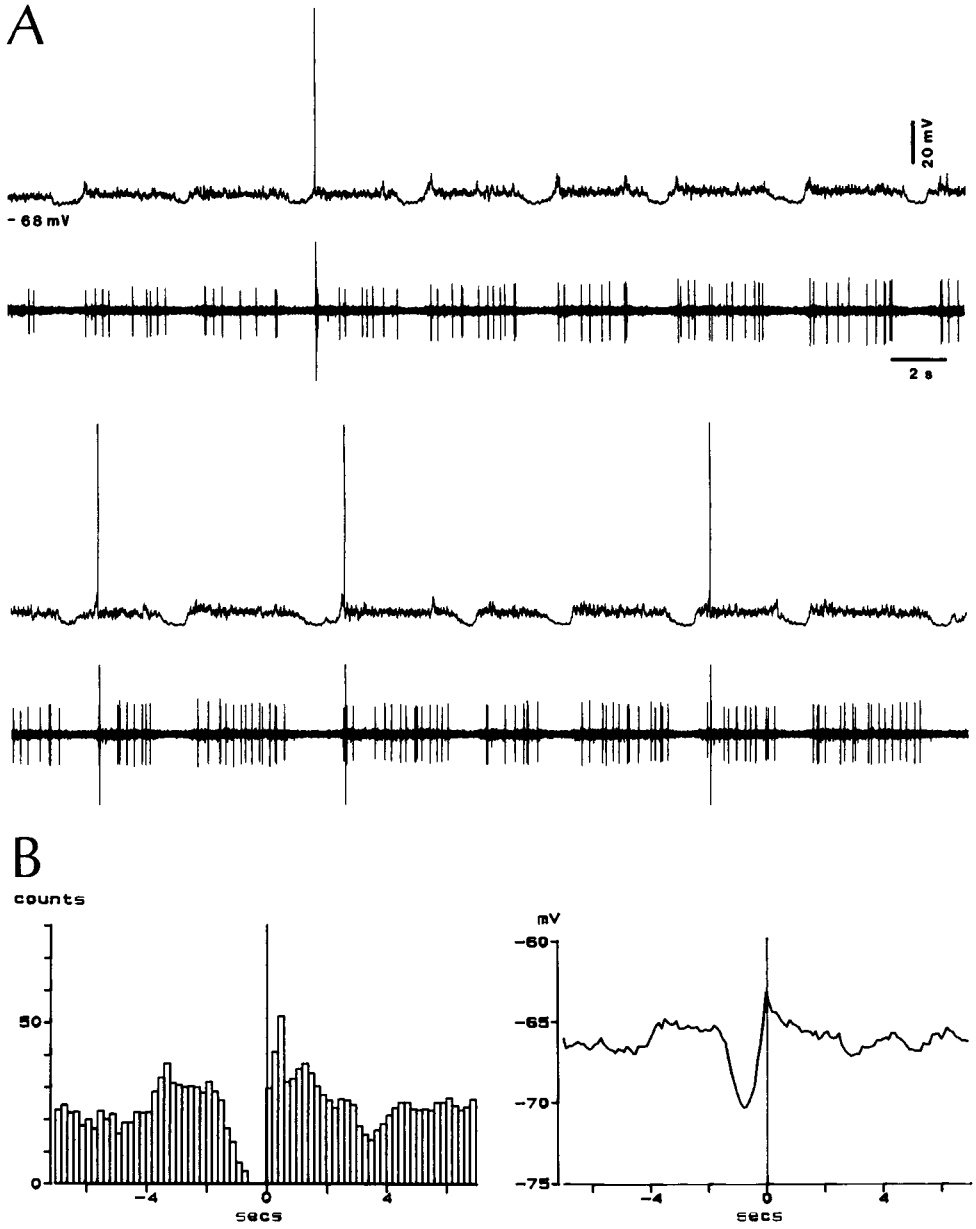

Figure 7. Synchronized inhibitions sculpturing the slow (≈0.2 Hz) oscillation in two simultaneously recorded cells at 1.5 mm in area 5. *A*, Uninterrupted recording, with *upper traces* depicting the intracellularly recorded cell and *lower traces* (increased gain in AC; intracellular action potential truncated) depicting the neuron recorded across the membrane. Note close time relation between hyperpolarizations and periods of silenced firing in the neighboring cell. *B*, Correlations between the inhibitory phases in the two cells. Correlations were computed between reference times established at the first spike in the extracellularly recorded neuron, following 30 silent periods of at least 0.5 sec, and all extracellularly recorded spikes (*left*) or intracellular potentials (*right*).

motor areas 4 and 6 and visual areas 17 and 18. The slow oscillation was present in 18 out of 25 motor cortical cells and in 15 out of 19 visual cortex cells. Figure 9 shows a neuron recorded in the posteromedial part of the marginal gyrus, at a depth of 0.8 mm in area 17, that responded to flashes of light with successive depolarizing–hyperpolarizing events and to dLGN stimulation with an EPSP–IPSP sequence starting at 2 msec (Fig. 9*A,B*). This cell oscillated at 0.3 Hz (Fig. 9*C,D*), indistinguishably from the majority of neurons recorded in areas 5 and 7.

Intracellular staining of slowly oscillating cells

We have stained 21 cells recorded from areas 5 and 7 that were oscillating at 0.25–0.4 Hz, as the majority of all other recorded neocortical cells. Without exception, the LY-stained neurons were pyramidal shaped. Nineteen cells were regular-spiking, slow-adapting neurons, recorded from the lower part of layer II to layer VI; and two neurons were intrinsically bursting cells recorded in layer III and in layer V (see also Nuñez et al., 1993; Steriade et al., 1993a). We did not stain regular-spiking fast-adapting neurons.

Figure 10 illustrates the morphological features of associational cortical neurons displaying the slow rhythm; *A–C* depict three cells located in layer V, while *D* represents the dye coupling of two cells in the middle part of layer III after injection of one neuron. Invariably, the soma surface in layer V cells was around 430 μm^2, with the pyramid base of ≈18 μm and its height of ≈24 μm. The apical dendrite in one layer V cell (Fig. 10*A*) could be followed up to layer II in different planes of sections. The other two layer V neurons (Fig. 10*B,C*) displayed very rich dendritic arborizations, particularly in the basal arbor, which could be followed for ≈0.4 mm around the soma. All three layer V cells were regular-spiking slow-adapting elements. At variance, the injected cell in layer III, where dye coupling was ob-

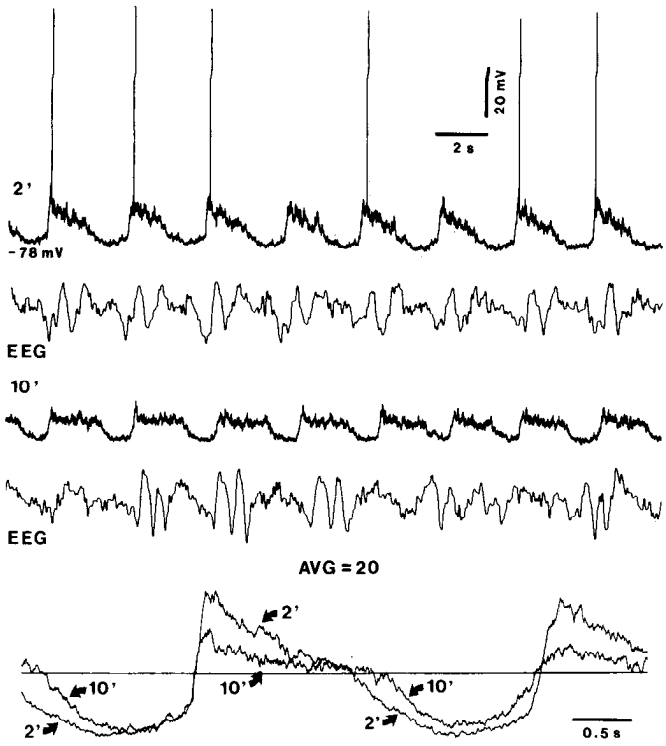

Figure 8. Decreased duration and amplitude of prolonged hyperpolarization after intracellular diffusion of Cl^-: neuron recorded at 0.8 mm in area 7. LP stimulus evoked an EPSP–IPSP sequence. The first component of the biphasic IPSP was reversed 8 min after impalement with a KCl-filled pipette (data not shown). Note, at 10 min (*10'*), diminished duration and amplitude of hyperpolarizations separating cyclic (≈0.3 Hz) depolarizations. The slow cellular rhythm and the EEG were not changed. The decreased steepness and amplitude of the initial component of the depolarization at 10 min after impalement are ascribed to the reduced hyperpolarization (diminution in the postinhibitory rebound component following the hyperpolarization). *Bottom*, Averages (*AVG*) of 20 expanded traces showing differences between depolarizations and hyperpolarizations at 2 min and 10 min after impalement.

tained (Fig. 10*D*), exhibited the typical electrophysiological characteristics of an intrinsically bursting neuron. The soma surface of the larger dye-coupled cell was ≈250 μm^2 (≈14 × 18 μm) and in the smaller neuron was ≈140 μm^2 (≈12 × 12 μm). Some of the secondary and tertiary branches of the apical dendrite in the larger layer III pyramid had numerous dendritic spines (right panel in Fig. 10*D*).

Discussion

The disclosure of a novel slow cortical rhythm in a very high proportion of cortical neurons is somehow surprising in view of the intensive investigations of neocortical neurons during the recent and more remote past. Probably, this rhythm was ignored in *in vivo* experiments because those studies focused on cellular responses to different sensory modalities and during motor performances, thus requiring alert preparations without slow oscillation of brain electrical activity. During the last decade, the results from *in vitro* cortical slices have achieved major breakthroughs in revealing a host of intrinsic and synaptic properties of various neuronal types in different cortical areas; inevitably, however, many dendrites are lopped when the slice is prepared and the whole cortical network is mutilated. As emphasized in an *in vitro* study (Chagnac-Amitai and Connors, 1989), small regions of the neocortex may sustain synchronous activity, but such limited circuits may not be adequate to support spontaneous oscillations for prolonged periods of time. The slow rhythm described in this article is a typical network-generated oscillation and, as shown in following articles (Steriade et al., 1993a,b), it results from the synchronous neuronal activities in close and distant cortical areas.

Note that the slow (<1 Hz) rhythms of thalamic and cortical systems have long been disregarded. Thalamic spindle waves (7–14 Hz) are grouped in sequences recurring with a slow (0.1–0.3 Hz) rhythm. The presence of this slow rhythm is clearly detectable in earlier EEG recordings, but it was only recently described with intracellular and field potential recordings (see Steriade et al., 1990b). On the other hand, EEG delta waves (1–4 Hz) were found to be grouped within sequences recurring every 8–12 sec (Oakson and Steriade, 1982; see also Fig. 1 in the present article). This slow rhythm was correlated with a similar rhythmicity of neurons recorded from midbrain reticular formation (Oakson and Steriade, 1982, 1983), but no further study of cellular substrates underlying the slow oscillation was undertaken. Cyclic groups of EEG delta waves at 3–4 Hz seem to recur in layers V–VI with a slow periodicity at 0.3–0.4 Hz (see Fig. 3*A* in Petsche et al., 1984), but the brevity of such periods in earlier studies prevented the disclosure and the detailed analysis of this slow rhythmicity. While the slow rhythm was not explicitly described in previous EEG studies of humans, groups of delta or other sleep waves recurring with a slow rhythmicity can be observed in earlier recordings performed during neurosurgery under local anesthesia (Henry and Scoville, 1952) or during sleep (e.g., Fig. 24 in Kellaway, 1990). Some of these slowly recurring wave sequences have previously been regarded as pathological, but a closer look led to the conclusion that they are "more likely to be a sign of health than of disease" (see Niedermeyer, 1987, p 193). This statement concerned the individual EEG waves; however, the clear-cut slow rhythm (0.25–0.3 Hz) of their sequences (see Fig. 14.12 in Niedermeyer, 1987) was not mentioned. We have recently analyzed this EEG oscillation during natural sleep in chronically implanted cats as well as during stages 3–4 of sleep in humans (Fig. 1).

The choice of anesthesia

The present recordings have been mostly performed under urethane anesthesia. Although the slow rhythm was shifted toward higher frequencies (0.6–1 Hz) under ketamine, instead of 0.3–0.4 Hz under urethane, the general characteristics of the oscillation were similar in these two anesthetic conditions. We did not use barbiturates because they produce an overwhelming picture of spindling, while obscuring other sleep rhythms. By contrast to the all-spindling pattern induced by barbiturates, unit and gross electrical activity under urethane anesthesia are more similar to those observed during late stages of natural slow-wave sleep in animals (Armstrong-James and Fox, 1984; Albrecht and Davidowa, 1989). Moreover, firing patterns and various electrophysiological parameters of cortical neurons under urethane anesthesia were found to be rather similar to those of cortical cells recorded in cortical slices, with the expected exception of a much higher apparent input resistance found *in vitro* (Bindman et al., 1988; Pollard and Angel, 1990).

While most experiments were conducted under urethane anesthesia, the slow rhythm was also observed by using other anesthetics. Moreover, it was present in undrugged preparations

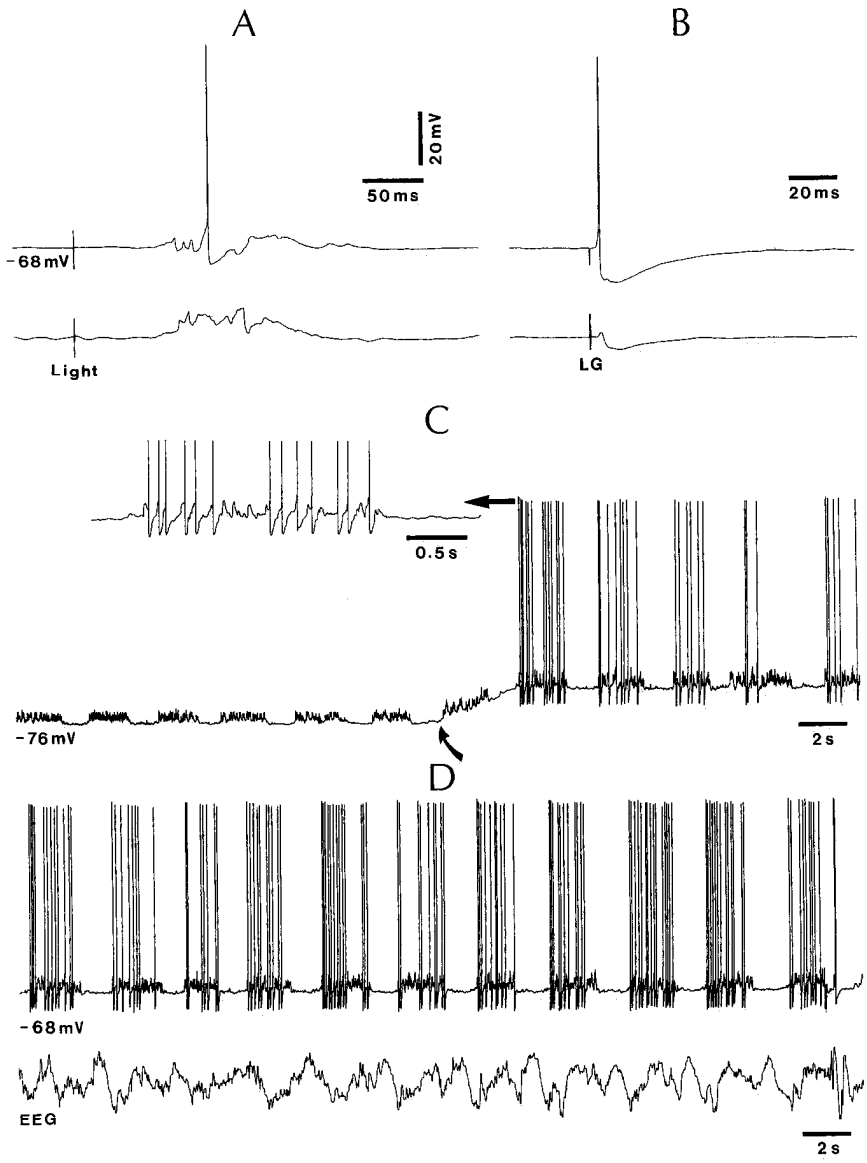

Figure 9. Slow oscillation (≈0.3 Hz) in primary visual cortex (area 17): neuron recorded at a depth of 0.8 mm. *A*, Two depolarizing responses to flashes of light (1 msec in duration). *B*, Responses to dLGN stimulation through two different stimulating electrodes: action potential generated in *upper trace*; pure EPSP–IPSP sequence in *bottom trace*. *C*, Spontaneous activity under −0.2 nA DC current and, at *oblique arrow*, back to the resting V_m (−68 mV). The first spike train is expanded at *left* (see *arrow*; spikes truncated). *D*, Relation of slow cellular oscillation with EEG activity recorded 2 mm rostral from the recorded site.

with transections at high collicular level (see Fig. 9 in Steriade et al., 1993a) as well as in chronically implanted, naturally sleeping animals (Fig. 1; M. Steriade, A. Nuñez, and F. Amzica, unpublished observations).

Excitatory events: partial spikes and slow depolarizing waves

The rhythmic spike trains were a conspicuous component of the slow cortical rhythm. Such a high level of excitatory activity would not be expected during a deep anesthetic state if the cortex were driven from the outside world. The main origin of this rhythmic depolarizations should be searched within the ipsilateral cortex itself, as similar oscillatory aspects were found after total destruction of thalamic perikarya projecting to areas 5 and 7, combined with callosotomy (see Figs. 10–12 in Steriade et al., 1993a).

The association suprasylvian areas 5 and 7 of cat display a wide convergent response pattern from various sensory modalities (Olausson et al., 1990). In addition to major inputs from LP, CL intralaminar, and posterior thalamic nuclei (Tanji et al., 1978; Graybiel and Berson, 1980; Steriade and Glenn, 1982; Avendaño et al., 1985), the afferents to cortical areas 5 and 7 include projections from somatosensory (Jones and Powell, 1969), visual (Kawamura, 1973), and cingulate limbic (Reinoso-Suarez, 1984) ipsilateral cortical areas. The main target of converging inputs from thalamic and cortical sources is the dendritic arbor of cortical neurons. All pyramidal-shaped as well as intrinsic spiny or nonspiny neurons with dendrites in a layer of thalamic termination may be contacted by asymmetric synapses of thalamic origin (Peters et al., 1976; White and Rock, 1981; White, 1986). Thalamic synapses are merely a minority of the asymmetric population of different types of long-axoned cortical cells, the intrinsic cortical input being prevalent. The dendritic site of convergence between thalamic and callosal inputs onto the same cortical cell is depicted in Figure 2*A* and is discussed below. Our data reported a high proportion of FPPs, possibly dendritic spikes, in slowly oscillating cortical neurons. Similar fast all-or-none events have been previously described in cortical and thalamic cells (e.g., Spencer and Kandel, 1961; Maekawa and Purpura, 1967; Paré et al., 1990; Pockberger, 1991).

As to the slow depolarizing envelope made up by short PSPs

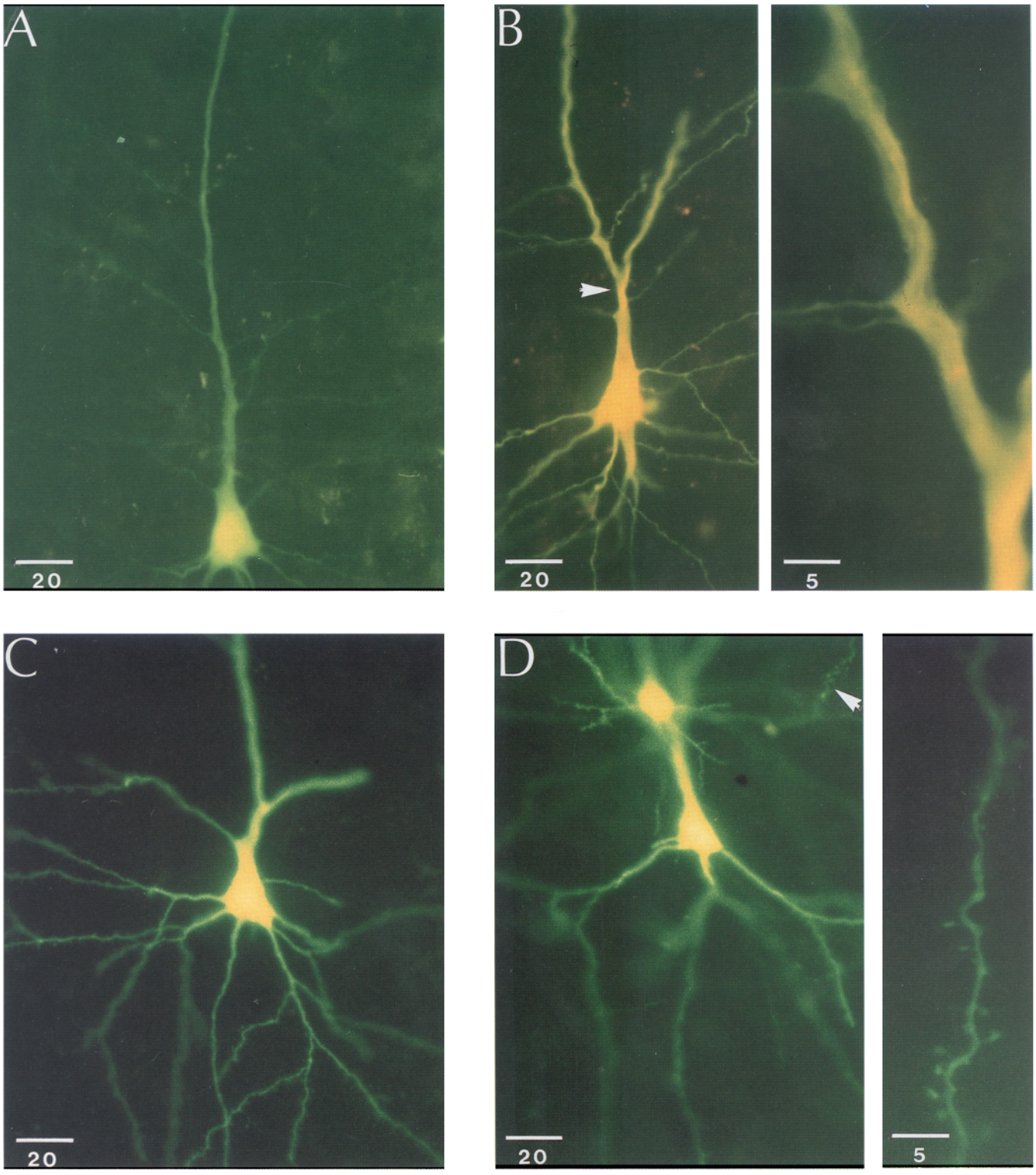

Figure 10. Soma shapes and dendritic arborizations of four slowly oscillating (0.25–0.4 Hz) pyramidal neurons recorded from areas 5 and 7. *A*, Regular-spiking, slow-adapting cell at a depth of 1 mm in area 7, with CL-evoked EPSP (2 msec latency). *B*, Regular-spiking, slow-adapting cell at a depth of 0.8 mm in area 5, antidromically identified from the CL (3 msec) and LP (4 msec) thalamic nuclei, and driven from the contralateral area 5 with an EPSP (6 msec). This neuron triggered a low-threshold spike when depolarized from −120 mV. Bifurcation of the apical dendrite (*arrow*) is expanded at *right*. *C*, Regular-spiking, slow-adapting cell at a depth of 0.9 mm in area 7: EPSPs driven from LP (15 msec) and CL (10 msec) thalamic nuclei. *D*, Dye coupling following LY injection in a single cell: radially arranged neurons, at a depth of ≈0.5 mm in area 5. The cell that was injected displayed intrinsic bursts by depolarizing current pulses and was driven with EPSPs from the LP (2 msec) and CL (2.5 msec) thalamic nuclei. *Arrow* points to a dendrite of larger-size (deeper-located) neuron, which is expanded at *right* to illustrate the dendritic spines. In all panels, *horizontal bars* indicate micrometers.

and full or partial spikes, our data suggest that both $g_{Na(p)}$ and NMDA-mediated EPSPs contribute to this prolonged depolarization. Probably, both the above mechanisms conjointly underlie the prolonged depolarization as, in most neurons, neither QX-314 nor ketamine alone were able to block this slow component completely.

In the majority of neurons, the amplitude of prolonged depolarizing wave was enhanced with DC hyperpolarizing current up to −90 mV (Fig. 3*B*). This is possibly accounted for by enhanced amplitudes of repetitive non-NMDA-mediated EPSPs and reversed IPSPs. We succeeded in suppressing the slow depolarization by DC hyperpolarizing current bringing the V_m to about −100 mV or at more negative values (Fig. 4). However, this was achieved less often, partly because we could not obtain stable recordings at such V_m levels in all cells.

The voltage-dependent, Mg^{2+}-sensitive, NMDA-mediated EPSPs were described in slices from various cortical areas and were evoked by stimulation of underlying white matter, cortical layers neighboring to the impaled cell, or corpus callosum (Thomson, 1986; Deisz et al., 1991; MacDonald et al., 1991; Sutor and Hablitz, 1989a,b). In our *in vivo* studies of association areas 5 and 7 cells (Nuñez et al., 1993), we detected the presence of two different components in thalamically or cortically evoked EPSPs, the late one building up incremental repetitive responses of the augmenting or recruiting type. During steady hyperpolarization, the amplitude of the early, short-lasting component of the EPSP increased, whereas the late depolarizing component (appearing at a latency of ≈20 msec) decreased and was eventually suppressed, thus suggesting its NMDA mediation. The present recordings showed that ketamine, a potent blocker of NMDA receptors (MacDonald et al., 1991), significantly reduced the duration of the depolarizing envelope. Although ketamine was administered systemically and thus could also act at thalamocortical synapses, its effect at the level of intrinsic cortical networks is indicated by the fact that the slow cortical rhythm survives complete destruction of thalamic perikarya projecting to suprasylvian areas 5 and 7 (see Figs. 10, 11 in Steriade et al., 1993a).

Inhibitory components: IPSPs and long-lasting hyperpolarizations

The high neuronal percentage (close to a fifth of oscillating cells) displaying grouped, repetitive IPSPs, recurring in cyclic sequences within the slow rhythm, indicates that local-circuit GABAergic neurons are part of the oscillating cortical network. It is known that neocortical neurons display IPSPs arising from an increase in Cl^- and K^+ conductances, mediated by $GABA_A$ and $GABA_B$ receptors, respectively (Kelly et al., 1969; Connors et al., 1982, 1988; Avoli, 1986; McCormick, 1989). The participation of local-circuit inhibitory cells in slow or fast rhythms, the frequency entrainment of postsynaptic oscillating pyramidal-type neurons, and the effects exerted by these interactions on large neuronal populations were modeled in both allo- and neocortex (Traub et al., 1989; Pedley and Traub, 1990; Lytton and Sejnowski, 1991; Wilson and Bower, 1992).

As to the prolonged hyperpolarizations separating the long-lasting depolarizing envelopes, the contribution of activities mediated by $GABA_A$ receptors linked with Cl^- channels is suggested by the results of Cl^- intracellular diffusion. The effect consisted in a reduction of amplitude and duration of prolonged periods of hyperpolarizations sculpturing the activity of cortical cells into the slow rhythm. The slowly developing Ca^{2+}-dependent K^+ current (Schwindt et al., 1988, 1992) is probably another major factor in the genesis of this component of the slow oscillation. Two sets of results support this assumption: (1) the amplitude of the hyperpolarizing phase decreased in parallel with the diminished duration of the slow depolarization after ketamine administration (Fig. 5), and (2) in cases when the slow oscillation mainly consisted of rhythmic hyperpolarizations sculpturing the background firing of cortical neurons, stimulation of brainstem cholinergic nuclei selectively suppressed the hyperpolarizing episodes, an effect sensitive to muscarinic blockers (Amzica et al., 1992). It is known that ACh blocks the Ca^{2+}-dependent and other K^+ currents in neocortex (see McCormick, 1992).

Morphological features of slowly oscillating cortical cells

All intracellularly stained, oscillating neurons in areas 5 and 7 were pyramidal-shaped cells from layers III–VI. This corroborates our inability to record fast-spiking elements, thought to be GABAergic stellate interneurons (McCormick et al., 1985). The electrophysiological analysis of stained cells showed their regular-spiking or intrinsically bursting characteristics. A study specifically directed to analyze the morphological differences between these two cell classes in layer V of rat neocortex (Chagnac-Amitai et al., 1990) reported that bursting cells have large pyramidal somata and an extensive basal and apical dendritic tree, whereas regular-spiking neurons have a more rounded soma and a smaller dendritic arborization. Although we only stained 2 intrinsically bursting cells out of the 21 cell sample, one of those cells was found in layer V and the other in layer III.

The dye coupling after intracellular LY injection into a single cell (Fig. 10*D*) resulted in a radial arrangement, with the bottom cell (probably the injected one) lying about 0.5 mm from the pia, and the upper neuron at ≈50 μm apart, within the same layer III. To our knowledge, neuronal dye coupling was until now revealed in electrophysiological experiments on only rat and guinea pig neocortex. Data showing basically identical radial arrangements and location in layer III, as described here, have been reported from sensorimotor cortical slices of rodents (Gutnick and Prince, 1981; Connors and Gutnick, 1984). It seems that the extent of coupling varies between cortical areas, species, and developmental periods. There is a dramatic reduction in coupling rates in ontogenesis, from 70% at 1–4 d to 30–40% by 10–15 d, down to 20% in the mature rat (Connors et al., 1983). Recent studies in the developing neocortex of rats showed radially oriented clusters of as many as 15–78 cells stained in the immediate vicinity of *one* injected neuron and suggested that, during early development, gap junctions could enable cortical cells by a direct, nonsynaptic mechanism (Yuste et al., 1992). The very rare occurrence of dye coupling in the adult cat, reported in the present article, is in line with the above data. The unequivocal morphological substrate of interneuronal coupling, the gap junction, was observed in the rat neocortex (Peters, 1980) and the sensorimotor cortex of the adult monkey, between the dendrites and soma of the "large stellate" neurons (Sloper, 1972; Sloper and Powell, 1978). The dye coupling between pyramidal-shaped neurons, as reported in previous experiments on rodent neocortex and in the present experiments on cat association neocortex, may be a basis for electrical synchronization, the more as previous *in vitro* studies on guinea pig and rat have provided evidence for antidromically elicited small sub-

threshold depolarizations and lack of collision with preceding orthodromic spikes in dye-coupled cells (Gutnick and Prince, 1981; Connors et al., 1983).

Concluding remarks

The high proportion of oscillating neurons (88%), their presence in distant and functionally different cortical areas, the morphological and electrophysiological identification of slowly rhythmic cells as pyramidal elements with thalamic and callosal projections, and the evidence of repetitive IPSPs grouped in sequences recurring at the same slow rhythm indicate that an overwhelming majority of cortical long-axoned cells as well as at least some of local-circuit inhibitory neurons are together involved in the genesis of this oscillation. All electrophysiological features of the slow rhythm emphasize that it emerges as a property of neocortical networks. The combined expression of EPSPs and IPSPs as well as the intrinsic currents of neocortical cells may vary according to the power of incoming depolarizing influences that depend on the degree of network synchronization, the position of a given cell in the cortical microcircuitry of pyramidal and local-circuit inhibitory neurons, and the distribution of $GABA_{A\text{-}B}$ receptors on the somadendritic membrane. These variables are further discussed, together with the corticothalamic interactions, in the final article of this series (Steriade et al., 1993b). The following articles will indeed demonstrate that the slow cellular oscillation in the cortex is dramatically synchronous with slow focal waves in various layers, with surface EEG potentials, as well as with EThG, and that it has a decisive role in synchronizing within this slow frequency range ($\approx$0.3 Hz) the previously known sleep rhythms, delta and spindle waves.

References

Albrecht D, Davidowa H (1989) Action of urethane on dorsal lateral geniculate neurons. Brain Res Bull 22:923–927.

Amzica F, Nuñez A, Steriade M (1992) Cholinergic and noradrenergic modulation of a slow oscillation in cat neocortical cells. Soc Neurosci Abstr 18:976.

Armstrong-James M, Fox K (1984) Similarities in unitary cortical activity between slow-wave sleep and light urethane anesthesia in the rat. J Physiol (Lond) 346:55P.

Avendaño C, Rausell E, Reinoso-Suarez F (1985) Thalamic projections to areas 5a and 5b of the parietal cortex in the cat: a retrograde horseradish peroxidase study. J Neurosci 5:1446–1470.

Avoli M (1986) Inhibitory potentials in neurons of the deep layers of the *in vitro* neocortical slice. Brain Res 370:165–170.

Avoli M, Olivier A (1989) Electrophysiological properties and synaptic responses in the deep layers of the human epileptogenic neocortex *in vitro*. J Neurophysiol 61:589–606.

Bindman LJ, Meyer T, Prince CA (1988) Comparison of the electrical properties of neocortical neurones in slices *in vitro* and in the anaesthetized rat. Exp Brain Res 69:489–496.

Chagnac-Amitai Y, Connors BW (1989) Synchronized excitation and inhibition driven by intrinsically bursting neurons in neocortex. J Neurophysiol 62:1149–1162.

Chagnac-Amitai Y, Luhmann HJ, Prince DA (1990) Burst generating and regular spiking layer 5 pyramidal neurons of rat neocortex have different morphological features. J Comp Neurol 296:598–613.

Connors BW, Gutnick MJ (1984) Neocortex: cellular properties and intrinsic circuitry. In: Brain slices (Dingledine R, ed), pp 313–338. New York: Plenum.

Connors BW, Gutnick MJ, Prince DA (1982) Electrophysiological properties of neocortical neurons *in vitro*. J Neurophysiol 48:1302–1320.

Connors BW, Benardo LS, Prince DA (1983) Coupling between neurons of the developing rat neocortex. J Neurosci 3:773–782.

Connors BW, Malenka RC, Silva LR (1988) Two inhibitory postsynaptic potentials, and $GABA_A$ and $GABA_B$ receptor-mediated responses in neocortex of rat and cat. J Physiol (Lond) 406:443–468.

Curró Dossi R, Nuñez A, Steriade M (1992) Electrophysiology of a slow (0.5–4 Hz) intrinsic oscillation of cat thalamocortical neurons *in vivo*. J Physiol (Lond) 447:215–234.

Deisz RA, Fortin G, Zieglgänsberger W (1991) Voltage dependence of excitatory postsynaptic potentials of rat neocortical neurons. J Neurophysiol 65:371–382.

Foehring RC, Lorenzon NM, Herron P, Wilson CJ (1991) Correlation of physiologically and morphologically identified neuronal types in human association cortex *in vitro*. J Neurophysiol 66:1825–1837.

Graybiel AM, Berson DM (1980) Histochemical identification and afferent connections of subdivisions in the lateral posterior-pulvinar complex and related thalamic nuclei in the cat. Neuroscience 5:1175–1238.

Gurewitsch M, Chatschaturian A (1928) Zur Cytoarchitektonik der Grosshirnrinde der Feliden. Z Anat Entwicklungsgesch 87:100–138.

Gutnick MJ, Prince DA (1981) Dye coupling and possible electrotonic coupling in the guinea pig neocortical slices. Science 211:67–70.

Hassler R, Muhs-Clement K (1964) Architektonischer Aufbau des sensomotorischen and parietalen Cortex der Katze. J Hirnforsch 6:377–420.

Henry CE, Scoville WB (1952) Suppression-burst activity from isolated cerebral cortex in man. Electroencephalogr Clin Neurophysiol 4:1–22.

Jones EG, Powell TPS (1969) Connexions of the somatic sensory cortex of the rhesus monkey. Brain 92:477–502.

Kawamura K (1973) Cortico-cortical fiber connections of the cat cerebrum. II. The parietal region. Brain Res 51:23–40.

Kellaway P (1990) An orderly approach to visual analysis: characteristics of the normal EEG of adults and children. In: Current practice of clinical electroencephalography (Daly DD, Pedley TA, eds), pp 139–199. New York: Raven.

Kelly JS, Krnjević K, Morris ME, Yim GKW (1969) Anionic permeability of cortical neurones. Exp Brain Res 7:11–31.

Leresche N, Lightowler S, Soltesz I, Jassik-Gerschenfeld D, Crunelli V (1991) Low-frequency oscillatory activities intrinsic to rat and cat thalamocortical cells. J Physiol (Lond) 441:155–174.

Lytton WW, Sejnowski TJ (1991) Simulations of cortical pyramidal neurons synchronized by inhibitory interneurons. J Neurophysiol 66:1059–1079.

MacDonald JF, Bartlett MC, Mody I, Pahapill P, Reynolds JN, Salter MW, Schneiderman JH, Pennefather PS (1991) Actions of ketamine, phencyclidine and MK-801 on NMDA receptor currents in cultured mouse hippocampal neurones. J Physiol (Lond) 432:483–508.

Maekawa K, Purpura DP (1967) Properties of spontaneous and evoked synaptic activities of thalamic ventrobasal neurons. J Neurophysiol 30:360–381.

McCormick DA (1989) GABA as an inhibitory neurotransmitter in human cerebral cortex. J Neurophysiol 62:1018–1027.

McCormick DA (1992) Neurotransmitter actions in the thalamus and cerebral cortex and their role in neuromodulation of thalamocortical activity. Prog Neurobiol 39:337–388.

McCormick DA, Pape HC (1990) Properties of a hyperpolarization-activated cation current and its role in rhythmic oscillation in thalamocortical neurones. J Physiol (Lond) 431:291–318.

McCormick DA, Connors BW, Lighthall JW, Prince DA (1985) Comparative electrophysiology of pyramidal and sparsely spiny stellate neurons of the neocortex. J Neurophysiol 54:782–806.

Niedermeyer E (1987) Abnormal EEG patterns (epileptic and paroxysmal). In: Electroencephalography, basic principles, clinical applications and related fields (Niedermeyer E, Lopes da Silva F, eds), pp 184–207. Baltimore: Urban and Schwartzenberg.

Nuñez A, Amzica F, Steriade M (1993) Electrophysiology of association cortical neurons *in vivo*: intrinsic properties and synaptic responses. J Neurophysiol, in press.

Oakson G, Steriade M (1982) Slow rhythmic rate fluctuations of cat midbrain reticular neurons in synchronized sleep and waking. Brain Res 247:277–288.

Oakson G, Steriade M (1983) Slow rhythmic oscillations of EEG slow-wave amplitudes and their relations to midbrain reticular discharge. Brain Res 269:386–390.

Olausson B, Shyu BC, Rydenhag B (1990) Properties of single neurons in the cat midsuprasylvian gyrus. Exp Brain Res 79:515–529.

Paré D, Steriade M, Deschênes M, Bouhassira D (1990) Prolonged

enhancement of anterior thalamic synaptic responsiveness by stimulation of a brainstem cholinergic group. J Neurosci 10:20–33.
Pedley TA, Traub RD (1990) Physiological basis of EEG. In: Current practice of clinical electroencephalography (Daly DD, Pedley TA, eds), pp 107–137. New York: Raven.
Peters A (1980) Morphological correlates of epilepsy: cells in the cerebral cortex. In: Antiepileptic drugs: mechanisms of action (Glaser GH, Penry JK, Woodbury DM, eds), pp 21–48. New York: Raven.
Peters A, Feldman M, Saldanha J (1976) The projection of the lateral geniculate nucleus on area 17 of the rat cerebral cortex. II. Terminations upon perikarya and dendritic shafts. J Neurocytol 5:85–107.
Petsche H, Pockberger H, Rappelsberger P (1984) On the search for the sources of the electroencephalogram. Neuroscience 11:1–27.
Pockberger H (1991) Electrophysiological and morphological properties of rat motor cortex neurons *in vivo*. Brain Res 539:181–190.
Pollard CE, Angel A (1990) Spontaneous single cell discharge in rat somatosensory cortical slices and its relationship to discharge in the urethane-anesthetized rat. Brain Res 518:120–126.
Reinoso-Suarez F (1984) Connectional patterns in parietotemporooccipital association cortex of the feline cerebral cortex. In: Cortical integration (Reinoso-Suarez F, Ajmone-Marsan C, eds), pp 255–278. New York: Raven.
Schwindt PC, Spain JW, Foehring RC, Stafstrom CE, Chubb MC, Crill WE (1988) Multiple potassium conductances and their functions in neurons from cat sensorimotor cortex *in vitro*. J Neurophysiol 59: 424–449.
Schwindt PC, Spain WJ, Crill WE (1992) Calcium-dependent potassium currents in neurons from cat sensorimotor cortex. J Neurophysiol 67:216–226.
Sloper JJ (1972) Gap junctions between dendrites in primate neocortex. Brain Res 44:641–646.
Sloper JJ, Powell TPS (1978) Gap junctions between dendrites and somata of neurons in primate sensori-motor cortex. Proc R Soc Lond [Biol] 203:39–47.
Spencer WA, Kandel ER (1961) Electrophysiology of hippocampal neurons. IV. Fast prepotentials. J Neurophysiol 24:272–285.
Stafstrom CE, Schwindt PC, Flatman JA, Crill WE (1985) Properties of persistent sodium conductance and calcium conductance of layer V neurons from cat sensorimotor cortex *in vitro*. J Neurophysiol 53: 153–170.
Steriade M, Glenn LL (1982) Neocortical and caudate projections of intralaminar thalamic neurons and their synaptic excitation from the midbrain reticular core. J Neurophysiol 48:352–371.
Steriade M, Gloor P, Llinás RR, Lopes da Silva F, Mesulam MM (1990a) Basic mechanisms of cerebral rhythmic activities. Electroencephalogr Clin Neurophysiol 76:481–508.
Steriade M, Jones EG, Llinás RR (1990b) Thalamic oscillations and signaling. New York: Wiley.
Steriade M, Curró Dossi R, Nuñez A (1991) Network modulation of a slow intrinsic oscillation of cat thalamocortical neurons implicated in sleep delta waves: cortically-induced synchronization and brainstem cholinergic suppression. J Neurosci 11:3200–3217.
Steriade M, Nuñez A, Amzica F (1993a) Intracellular analysis of relations between the slow (<1 Hz) neocortical oscillation and other sleep rhythms of the electroencephalogram. J Neurosci 13:3266–3283.
Steriade M, Contreras D, Curró Dossi R, Nuñez A (1993b) The slow (<1 Hz) oscillation in reticular thalamic and thalamocortical neurons: scenario of sleep rhythm generation in interacting thalamic and neocortical networks. J Neurosci 13:3284–3299.
Sutor B, Hablitz JJ (1989a) EPSPs in rat neocortical neurons *in vitro*. I. Electrophysiological evidence for two distinct EPSPs. J Neurophysiol 61:607–620.
Sutor B, Hablitz JJ (1989b) EPSPs in rat neocortical neurons *in vitro*. II. Involvement of *N*-methyl-D-aspartate receptors in the generation of EPSPs. J Neurophysiol 61:621–634.
Tanji DG, Wise SP, Dykes RW, Jones EG (1978) Cytoarchitecture and thalamic connectivity of third somatosensory area of cat cerebral cortex. J Neurophysiol 41:268–284.
Thomson AM (1986) A magnesium-sensitive post-synaptic potential in rat cerebral cortex resembles neuronal responses to *N*-methylaspartate. J Physiol (Lond) 370:531–549.
Traub RD, Miles R, Wong RKS (1989) Model of the origin of rhythmic population oscillations in the hippocampal slice. Science 243:1319–1325.
White EL (1986) Termination of thalamic afferents in the cerebral cortex. In: Cerebral cortex, Vol 5 (Jones EG, Peters A, eds), pp 271–289. New York: Plenum.
White EL, Rock MP (1981) A comparison of thalamocortical and other synaptic inputs to dendrites of two non-spiny neurons in a single barrel of mouse SmI cortex. J Comp Neurol 195:265–277.
Wilson M, Bower JM (1992) Cortical oscillations and temporal interactions in a computer simulation of piriform cortex. J Neurophysiol 67:981–995.
Yuste R, Peinado A, Katz LC (1992) Neuronal domains in developing neocortex. Science 257:665–669.